Single-Frequency, Single-Spatial-Mode ROW-DFB Diode Laser Arrays

M. P. Nesnidal, L. J. Mawst, *Senior Member, IEEE,* A. Bhattacharya, D. Botez, *Fellow, IEEE,* L. DiMarco, J. C. Connolly, *Member, IEEE,* and J. H. Abeles, *Member, IEEE*

Abstract— **Single-frequency, stable single-spatial-mode operation from large-aperture (40–60 μm) index-guided devices is demonstrated from resonant antiguided phase-locked InGaAs–InGaP–GaAs diode-laser arrays incorporating 2nd-order distributed-feedback gratings (i.e., ROW-DFB arrays). The devices operate in a single-spatial-mode up to 3.6 × threshold, and truly single-mode (i.e., single-spatial-mode and single-frequency) up to 2 × threshold. For 40 (60)-μm-aperture 10-element arrays, the beam pattern is in-phase and diffraction-limited with 70% (75%) of the power residing in the main lobe. Single-frequency operation is obtained from 9640–9652 Å, over a temperature range of approximately 20 °C, . Side-mode suppression ratios ≥20 dB are recorded up to 2 × threshold.**

I. Introduction

HIGH-POWER, single-frequency, single-spatial-mode diode lasers are of fundamental importance for many applications such as coherent blue-light generation via frequency doubling for high-density optical memories, parallel optical-signal processing, free-space optical communications, and high-speed, high-resolution laser printing.

Conventional, narrow-stripe (3–4 μm), single-mode lasers have demonstrated at most 200 mW of reliable power [1]. Output power has been limited by the degradation of the facets and/or the onset of mode instability at high emitted-power densities. For reliable watt-range output power, devices possessing wide (≥50 μm) emitting apertures are necessary. However, single-stripe, large-aperture lasers are inherently multimodal since the number of lateral modes within a single stripe increases with aperture width. Recently, fanout-type master-oscillator power-amplifier (MOPA) devices of the "broad-area" type have displayed watts of diffraction-limited, single-frequency power [2]–[5]. However, broad-area MOPA devices possess inherent instabilities due to refractive index variations induced by thermal gradients and injected carriers [6]–[8]. The position of external spherical lenses required to achieve diffraction-limited, collimated beams is drive dependent [2]–[4]. These facts may explain why there have been no reliability data available for MOPA devices after more than three years from commercial introduction. Therefore, there is a clear need for large-aperture devices with strong built-in index guiding.

Previous attempts to obtain truly single-mode operation (i.e., single-frequency and single-spatial-mode) from positive-index-guided arrays employing distributed feedback (DFB) [9]–[11] relied on the belief that the DFB grating would provide (lateral) spatial-mode discrimination in addition to (longitudinal) frequency selection. That is, because the array modes adjacent to the fundamental mode correspond to pairs of flat phasefronts tilted with respect to the array axis, it was believed that the grating would act as a spatial-mode discriminator. K.-Y. Liou *et al.* [9] have demonstrated 12-element evanescent-wave-coupled arrays operating single-frequency, but in beam patterns with lobewidths in excess of 4 × diffraction limit (DL). Similarly, Miller *et al.* [10] obtained lobewidths 3.6 × DL from 14-element evanescent-wave-coupled devices, and Twu *et al.* [11] and Dong *et al.* [12], while using five-element devices, obtained lobewidths 2.5–3 × DL. That is, for phase-locked arrays, DFB structures do not, in general, act as (lateral) spatial-mode selectors. Mawst *et al.* [13] achieved single frequency, in-phase-mode operation from 10-element nonresonant antiguided arrays using Talbot filters to discriminate against out-of-phase modes. However, lack of adjacent-mode discrimination resulted in lobewidths 2 × DL. Only with the addition of a monolithic spatial filter were Dong *et al.* [12] able to achieve diffraction-limited spectra from evanescent-wave-coupled devices, but from relatively small apertures (i.e., 18 μm).

The goal of this work has been to demonstrate *stable* single-mode operation from large-aperture antiguided arrays. In this Letter, we present preliminary results from the first large-aperture (40–60 μm) index-guided diode lasers operating both single-frequency as well as in a stable, single spatial mode. Unoptimized devices provide truly single-mode operation to 2 × threshold and 50 mW output power. The resonant optical waveguide (ROW) array provides (lateral) spatial-mode selectivity, while the DFB grating structure, placed in close proximity to the active region, provides (longitudinal) frequency discrimination. ROW arrays possess large built-in index steps ($\Delta n \approx 0.05$) yielding a stable beam pattern essentially invulnerable to index variations due to thermal gradients and/or injected carriers [14]–[16]. As previously shown, the spatial-mode stability of such large-aperture devices has the potential for watt-range coherent output powers [14]–[16]. In addition, the concept is implemented in an aluminum-free InGaAs–InGaAsP–InGaP structure that eases device fabrication

Manuscript received September 22, 1995; revised October 26, 1995. This work was supported in part by the National Science Foundation under grant ECS-9411713.

M. P. Nesnidal, L. J. Mawst, A. Bhattacharya, and D. Botez are with the Electrical Engineering Department, University of Wisconsin-Madison, 1415 Engineering Drive, Madison, WI 53706 USA.

L. DiMarco, J. C. Connolly, and J. H. Abeles are with the David Sarnoff Research Laboratories, 201 Washington Road, Princeton, NJ 08543 USA.

Publisher Item Identifier S 1041-1135(96)00930-5.

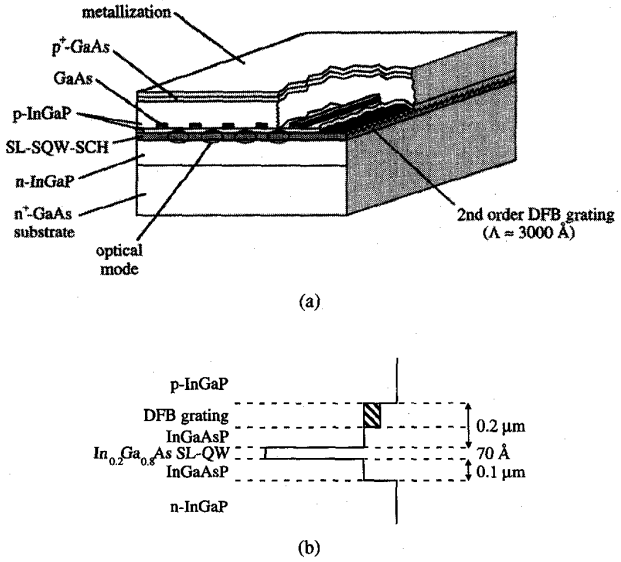

Fig. 1. (a) Schematic representation of ROW-DFB array. The lateral array structure, designed such that the in-phase mode is resonant, provides spatial-mode selection while the longitudinal 2nd-order DFB grating provides frequency selection. 150-Å-thick $In_{0.2}Ga_{0.8}As$ quantum wells centered within the GaAs guides provide interelement loss. (b) Energy band schematic of the SL-SQW-SCH structure.

and ensures long-term reliability. In contrast, fabrication of AlGaAs–GaAs DFB structures has been a difficult problem due to defects that occur while regrowing over inherently oxidized aluminum-containing layers.

It should be noted that evanescent-wave-coupled devices operating in-phase are generally limited to 5–7 elements [17] because, in devices with excess gain in the low-index regions, leaky modes are favored as the number of elements, $N \geq 7$. Therefore, for large-aperture (≥ 50 μm) index-guided devices, only antiguided arrays are a viable option.

II. Device Design and Fabrication

Epitaxial growth is performed in an Aixtron A-200 MOVPE reactor at 700 °C and 50 mbar. A schematic representation of the ROW-DFB array is shown in Fig. 1. A second-order DFB grating ($\Lambda \approx 3000$ Å) is defined holographically atop the upper InGaAsP confinement layer. A lossy 150 Å-thick InGaAs quantum well is grown within a GaAs guide layer to provide array-mode intermodal discrimination [14], [15]. The array is formed by preferentially etching regions including the GaAs (transverse) guide layer and InGaAs quantum well.

The 40 (60)-μm-aperture arrays demonstrated here consist of 10 elements of 3 (5)-μm-wide low-(effective)-index regions, and 1-μm-wide high-index GaAs guide regions. The array structures are designed such that the in-phase mode is resonant. The InGaAs quantum well within the GaAs guides provides interelement loss and effectively suppresses out-of-phase modes [15], thus eliminating the need for Talbot-type filters. The latter proved particularly troublesome in previous DFB devices [13], since the presence of the grating in the Talbot region prevented out-of-phase mode suppression.

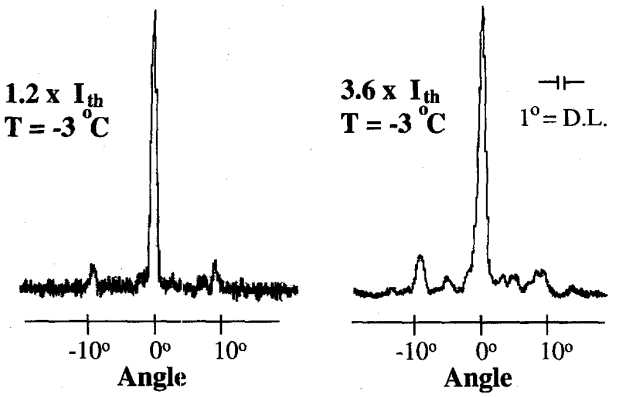

Fig. 2. Relative intensities of diffraction-limited, single-spatial-mode far-field patterns for 60-μm-aperture devices at two drive levels. I_{th} is the threshold current.

III. Results and Discussion

All devices are 1000 μm long and have no facet coatings. Diffraction-limited, far-field patterns for 60 μm-aperture devices are obtained up to 3.6 × threshold (Fig. 2). The diffraction-limited width of the main lobe is 1°, and 75% of the output power resides in the main lobe. Fig. 3 depicts the longitudinal-mode spectrum for various drive levels at a heat-sink temperature of approximately −3 °C. At a threshold current of 500 mA, single-frequency operation at 9586 Å is observed, with a side-mode suppression ratio of at least 25 dB. Single-frequency operation continues to twice threshold, where the side-mode suppression ratio reaches 18–20 dB. Additional longitudinal modes appear above twice threshold. DFB performance has been confirmed by recording a longitudinal-mode temperature dependence of 0.6 Å/°C over a 20 °C-wide range. The devices' performance is thus truly single-mode. Diffraction-limited, single-spatial-mode far-field patterns for 40 μm-aperture devices (up to 1.3 × threshold), and accompanying single-frequency-mode spectra were obtained at room temperature, and are similar to those in Figs. 2 and 3, respectively. Again, purely single-mode operation was observed. A diffraction-limited beam width of 1.4° was measured, and 70% of the output power resided in the main lobe. It should be noted that the longitudinal-mode spectra in Fig. 3 were measured near −3 °C, since grating optimization has not yet been achieved. For these arrays, the gain peak is at $\lambda \approx 0.98$ μm while DFB action occurs in the 0.965–0.969 μm range.

A spectrally-resolved near-field pattern for the 40-μm-aperture array is shown in Fig. 4. Single-frequency operation is again confirmed, and array-mode spatial uniformity is evident. The near-field uniformity reflects the parallel coupling in ROW arrays. Because the gain is used uniformly within the active region, high-order spatial modes do not appear, for 60-μm-aperture devices, up to at least 3.6 × threshold, the highest drive-level tested.

Typical thresholds were 500 mA for 60-μm-aperture, 1000-μm-long arrays. For these preliminary devices, maximum single-mode power for both types of arrays was only on the order of 50 mW. The relatively high threshold currents can be explained by the wavelength mismatch between the material

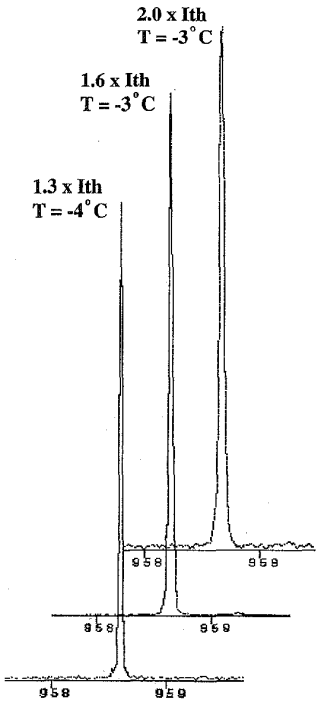

Fig. 3. Single-frequency spectra for 60-μm-aperture devices at various drive levels. The vertical scale is linear and represents the relative intensity.

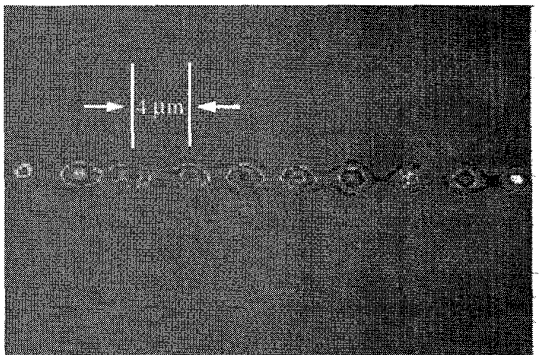

Fig. 4. Spectrally-resolved near-field pattern of a 40-μm-aperture device.

gain peak and the DFB grating resonance. The low output power reported can be attributed to two causes. First, the devices were relatively long (1 mm), and therefore, hampered by scattering losses. Second, since the second-order DFB grating was not optimized, radiation losses are quite likely to have diminished edge-emission lasing efficiency.

Improvements in device performance are therefore anticipated when the wavelength mismatch is minimized, and the device length and grating duty cycle are optimized. Furthermore, although single-mode operation has been demonstrated to twice threshold, the lack of facet coatings allows for the possibility of two-mode operation [12]. Asymmetric facet coatings (i.e., AR + HR) must therefore be applied to achieve maximum output power and insure single-frequency operation in a longitudinally uniform device. Thus, dramatic increases in coherent output power are expected with device optimization.

The use of ROW-DFB arrays removes the physical limitations imposed on aperture width for in-phase evanescent-wave coupled arrays. The ability to simultaneously satisfy both lateral and longitudinal resonance conditions has been demonstrated here for the first time for large-aperture (40–60 μm) index-guided devices.

REFERENCES

[1] A. Moser, A. Oosenberg, E. E. Latta, T. Forster, and M. Gasser, "High power operation of strained InGaAs/GaAs single quantum well lasers," *Appl. Phys. Lett.*, vol. 59, pp. 2642–2644, 1991.

[2] J. N. Walpole, E. S. Kintzer, S. R. Chinn, C. A. Wang, and L. J. Missaggia, "High-power strained-layer InGaAs/AlGaAs tapered traveling wave amplifier," *Appl. Phys. Lett.*, vol. 61, pp. 740–742, Aug. 1992.

[3] D. Mehuys, D. F. Welch, and L. Goldberg, "2.0 W CW, diffraction-limited tapered amplifier with diode injection," *Electron. Lett.*, vol. 28, pp. 1944–1946, Oct. 1992.

[4] D. F. Welch, R. Parke, D. Mehuys, A. Hardy, R. Lang, S. O'Brien, and D. Scifres, "1.1 W CW, diffraction-limited operation of a monolithically integrated flared-amplifier master oscillator power amplifier," *Electron. Lett.*, vol. 28, pp. 2011–2013, 1992.

[5] J. H. Abeles, R. Amantea, N. W. Carlson, J. T. Andrews, P. K. York, J. C. Connolly, R. Rios, W. F. Reichert, J. B. Kirk, T. J. Zamerowski, D. B. Gilbert, S. K. Liew, N. A. Hughes, J. K. Butler, G. Evans, S. Y. Narayan, and D. J. Channin, "Monolithic fanned-out amplifier-laser master oscillator power amplifiers," in *13th IEEE Int. Semiconductor Laser Conf.*, Takamatsu, Japan, Sept. 21–25, 1992, Paper PD-12.

[6] J. H. Abeles, R. Amantea, R. Rios, and D. J. Channin, "Finite difference beam propagation method modeling for high power fanned-out amplifier lasers," in *OSA Opt. Design Photon. Conf.*, Palm Springs, CA, Mar. 22–24, 1993, Paper PD-2.

[7] L. Goldberg, M. Surette, and D. Mehuys, "Filament formation in a tapered GaAlAs optical amplifier," *Appl. Phys. Lett.*, vol. 62, no. 5, pp. 2304–2306, 1993.

[8] S. Ramanujan and H.G. Winful, "Suppression of filamentation in flared amplifiers," in *OSA-IPR '95 Conf.*, Dana Point, CA, Paper IFF-1, Feb. 23–25, 1995, pp. 254–256.

[9] K.-Y. Liou, A. G. Dentai, E. C. Burrows, R. P. Gnall, C. M. Joyner, and C. A. Burrus, "High-power multiple-quantum-well distributed feedback laser arrays and Fabry–Perot laser arrays at 1.5 μm wavelength," in *Tech. Dig. 13th IEEE Int. Semiconductor Laser Conf.*, Takamatsu, Japan, Sept. 21–25, 1992, Paper D-27, pp. 88–89.

[10] L. M. Miller, K. J. Beernink, J. T. Verdeyen, J. J. Coleman, J. S. Hughes, G. M. Smith, J. Honig, and T. M. Cockerill, "InGaAs–GaAs–AlGaAs strained-layer distributed feedback ridge waveguide quantum well heterostructure laser array," *Electron. Lett.*, vol. 27, pp. 1943–1945, 1991.

[11] Y. Twu, N. K. Dutta, C. A. Green, and J. D. Wynn, "GaInAsP distributed feedback laser array," *Electron. Lett.*, vol. 24, pp. 743–744, 1988.

[12] J. Dong, T. Ikeda, S. Arai, and K. Komori, "A GaInAsP/InP grating filter multiple-stripe laser array operating in in-phase lateral- and single-longitudinal-mode," *IEEE Photon. Technol. Lett.*, vol. 4, pp. 491–494, May, 1992.

[13] L. J. Mawst, C. Tu, C. Zmudzinski, and D. Botez, "Single-frequency antiguided laser array with buried distributed feedback grating," *J. Appl. Phys.*, vol. 75, pp. 7220–7223, 1994.

[14] D. Botez, M. Jansen, L. J. Mawst, G. Peterson, and T. J. Roth, "Watt-range, coherent uniphase powers from phase-locked arrays of antiguided diode lasers," *Appl. Phys. Lett.*, vol. 58, pp. 2070–2072, 1991.

[15] L. J. Mawst, D. Botez, C. A. Zmudzinski, M. Jansen, C. Tu, T. J. Roth, and J. Yun, "Resonant self-aligned-stripe antiguided diode laser arrays," *Appl. Phys. Lett.*, vol. 60, pp. 668–670, 1992.

[16] C. A. Zmudzinski, D. Botez, and L. J. Mawst, "Coherent one-watt operation of large-aperture resonant arrays of antiguided diode lasers," *Appl. Phys. Lett.*, vol. 62, pp. 2914–2916, 1993.

[17] H. Fujii, I. Suemune, and M. Yamanishi, "Analysis of transverse modes of phase-locked multi-stripe lasers," *Electron. Lett.*, vol. 21, no. 16, pp. 713–714, Aug. 1985.